5-9-2011

Hydrodynamic Modeling of Surface Plasmon Enhanced Photon Induced Current in a Gold Grating

Alex English
Boise State University

Cheng-Wen Cheng
Academia Sinica

Lloyd Lowe II
Boise State University

Min-Hsiung Shih
Academia Sinica

Wan Kuang
Boise State University

DOI: 10.1063/1.3590200

Hydrodynamic modeling of surface plasmon enhanced photon induced current in a gold grating

Alex English,[1] Cheng-Wen Cheng,[2,3,4] Lloyd Lowe II,[1] Min-Hsiung Shih,[2] and Wan Kuang[1,a)]

[1)] *Dept. of Electrical and Computer Engineering, Boise State University, Boise, ID 83725*

[2)] *Research Center for Applied Sciences, Academia Sinica, Taipei 11529, Taiwan*

[3)] *Taiwan International Graduate Program (TIGP), Academia Sinica, Taiwan*

[4)] *Department of Physics, National Taiwan University, Taipei 10617, Taiwan*

The current induced by incident photons on an gold grating slab is investigated numerically and experimentally. A semi-classical electrodynamic model is developed under the weak nonlinearity approximation. Electrons in the conduction band are treated as an electron gas in the presence of a self-consistent electromagnetic field. The model is solved by the finite element method and compared with measurements. The calculated current density as a function of incident angle and wavelength is found to be in qualitative agreement with the experimental measurements. The results show that increasing surface plasmon spatial variation enhances photon induced current.

Enhancement of optical properties, such as extraordinary transmission, by plasmon resonances in metallic materials has attracted much attention over the past two decades.[1,2] A great deal of the recent interest in these materials focuses on enhancing local electromagnetic fields to facilitate stronger light-matter interactions. Strong local fields are particularly important for nonlinear optical processes, which scale with electromagnetic field strength. A growing body of experimental studies of second-order nonlinearity has been reported.[3–11] While a light beam with the frequency of ω can induce both a second harmonic polarization as a result of $\omega+\omega=2\omega$ and a DC polarization as a result of $\omega-\omega=0$, the latter effect has received far less attention. DC polarization has many applications, such as high-speed light detection and terahertz radiation generation.[11–13] It can also potentially be used in the investigation of electron dynamics in metallic nanostructures. Thus far, DC polarization has been described in terms of photons imparting their momentum to electrons and holes in conductive materials.[4,8,14] However, the recent observation of an enhanced photon induced voltage on an Au grating slab[8] compared to a prism-coupled flat Au film[4] suggests that the momentum conservation argument itself is insufficient to explain these measurements. In addition, experiments of second harmonic generation[7,15] on metallic metamaterials showed that the overall shape of the structures plays a significant role in determining nonlinear response. It is expected that a more complete understanding shall account for the spatial distribution of the electromagnetic field and the electron transport over nonuniform nanostructures.

In this Letter, the hydrodynamic theory developed by Goff and Schaich[16] for simple metals will be applied to structured metal slabs. The model is solved for an Au grating slab under the weak nonlinearity approximation using the finite element method (FEM) and compared with experimental measurements. The results of the numerical calculations agree qualitatively with the experimental results, indicating that spatially varying electromagnetic field strength plays a significant role in photon induced current.

The photon induced current can be treated by Maxwell's equations with an explicit current density $\boldsymbol{J}$,

$$\nabla\times\boldsymbol{H}(r,t)=\varepsilon_0\frac{\partial\boldsymbol{E}(r,t)}{\partial t}+\frac{\partial\boldsymbol{P}(r,t)}{\partial t}+\boldsymbol{J}(r,t), \qquad (1)$$

where $\boldsymbol{J}$ is due to electron transport in metal. The electric field $\boldsymbol{E}$ and polarization $\boldsymbol{P}$ in Eq. (1) are written out separately for numerical convenience. In the absence of interband transitions, the response of the conduction electrons to an external electromagnetic field may be calculated classically. The electrons in the conduction band can be treated as an electron gas with an effective mass m^* in the presence of the self-consistent fields $\boldsymbol{E}$ and $\boldsymbol{H}$.[17] The hydrodynamic equation of motion for the average velocity $\boldsymbol{v}(r,t)$ is given by,

$$\frac{\partial\boldsymbol{j}}{\partial t}+\boldsymbol{v}(\nabla\cdot\boldsymbol{j})+(\boldsymbol{j}\cdot\nabla)\boldsymbol{v}=\frac{e}{m^*}(n\boldsymbol{E}+\boldsymbol{j}\times\boldsymbol{B})-\frac{\nabla p}{m^*}-\frac{\boldsymbol{j}}{\tau_m}, \quad (2)$$

where $\boldsymbol{j}$ is electron flux density $\boldsymbol{j}=n\boldsymbol{v}$ and pressure p is attributed to quantum mechanical Coulomb correlations and exchange contribution, described by a Thomas-Fermi statistics, $p(\boldsymbol{r},t)=\zeta n^{5/3}(\boldsymbol{r},t)$, in which ζ is a constant $\zeta=3^5\hbar^2\pi^{4/3}/25m^*$.[18,19] A phenomenological decay time τ_m is employed to describe other Coulomb scattering. To calculate the nonlinear current density, all variables in Eq. (2) are expanded as a series of orders where $A=A_0+\tilde{A}_1e^{i\omega t}+\tilde{A}_2e^{2i\omega t}+\cdots$ and A is either $\boldsymbol{E}$, n, $\boldsymbol{j}$ or p. A_0 is the equilibrium value of the variable and $\tilde{A}_i$ are complex values. Solving Eq. (2) for the photon induced current,

$$\boldsymbol{j}_v=2\Re\left[\frac{e\tau_m}{m^*}\left(\tilde{n}_1^*\tilde{\boldsymbol{E}}_1+\tilde{\boldsymbol{j}}_1^*\times\tilde{\boldsymbol{B}}_1\right)-\tau_m\left(\nabla\cdot\tilde{\boldsymbol{j}}_1\right)\tilde{\boldsymbol{v}}_1^*-\tau_m\left(\tilde{\boldsymbol{j}}_1\cdot\nabla\right)\tilde{\boldsymbol{v}}_1^*\right]-\frac{10\tau_m\zeta}{9m^*}n_0^{-1/3}\nabla|\tilde{n}_1|^2 \qquad (3)$$

a)Electronic mail: wankuang@boisestate.edu

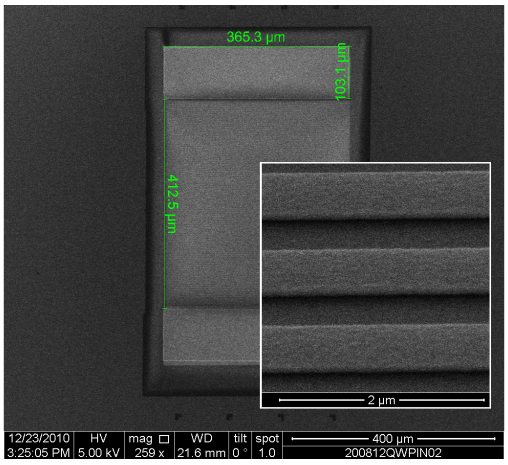

Figure 1. Scanning electron microscope image of a Au grating slab with dimensions labeled. The inset shows the details of the grating.

where $\Re[\cdot]$ denotes the real part of the expression.[20] Equation (3) was solved by the finite element method using the commercial software package COMSOL[21] in the general equation mode. The two-dimensional simulation was performed for single period of an infinitely wide grating slab with a Bloch-Floquet boundary condition and a perfectly matched layer boundary condition.[20] The simulation results will be discussed in comparison with the measurements.

Experimentally, the effect of a photon induced current can be measured as the voltage induced across the Au grating slab. Figure 1 shows the scanning electron microscope image of a fabricated Au grating slab. A 3 nm thick chromium adhesion layer was evaportated onto a silica substrate followed by evaporation of a 50 nm thick Au film. Periodic grooves with a 1.2 μm spacing were etched into the Au film by electron beam lithography and ion beam etching. The etching stopped short of completely removing the Au film to protect the Cr layer from oxidizing and also to provide a conductive path for displaced electrons. The structure is electrically isolated from the surrounding Au film. Electrical contacts were deposited at both ends of the grating slab and were wire bonded to a SMA connector. No RF impedance matching was attempted in the experiment. The total resistance as measured at the SMA connector was 48 Ω.

The incident light was produced from an optical parametric oscillator pumped by a frequency-tripled Q-switched YAG laser (OPOTek, Vibrant LD) whose wavelength was varied from 1 μm to 1.6 μm in the measurements. The induced voltage was fed to a 350 MHz amplifier (Standford Research Systems, SR445A) and measured by a 2.5 GHz digital storage oscilloscope (Agilent, Infinium DSO 90254A) triggered by the Q-switch of the laser. The laser beam was *p*-polarized and focused at the sample surface with a beam size of approximately 0.3 mm. The induced voltage was measured as a function of incident angle and wavelength. In all measurements, a ~0.2 ns increase in pulse width, or 10% with respect to the incident optical pulse, was observed.[20] We attribute the pulse broadening to a lack of impedance matching between the Au grating slab and the SMA connector.

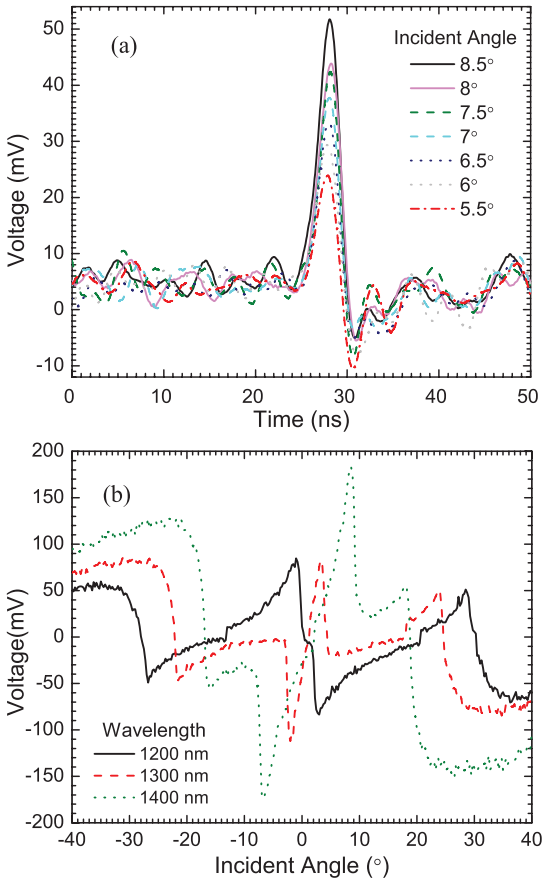

Figure 2. (a) Photon induced voltage on the Au grating slab for different incident angles at the incident wavelength of 1.2 μm. (b) The induced voltage peaks as a function of incident angle for the incident wavelengths of 1.2, 1.3, and 1.4 μm.

Figure 2(a) shows the photon induced voltage at the incident wavelength of 1.2 μm after amplified by a factor of 125. The noise floor was about 10 mV after the amplifier. The incident pulse energy was 2 μJ and the incident angle was varied from 5.5° to 8.5° in the measurement. No change in pulse width was observed. The maximal response achieved at 8.5° coincides with the excitation of surface plasmon resonance, as will be shown.

Figure 2(b) shows the peak voltage measured after the amplifier induced in the Au grating slab as a function of incident angle and wavelength. The direction of induced current reverses when the incident angle changes sign, consistent with a centro-symmetric structure. The peaks occurring between $\pm 15°$ in the figure are the result of surface plasmon resonance at the air and Au interface. At the incident wavelength of 1200 nm and 1300 nm, the surface plasmon resonance is excited by diffraction order -1 and 1, respectively.[20] Hence, the polarity of the photon induced voltage is expected to be reversed as shown in Fig. 2(b). Additional peaks observed at incident angles larger than 15° are due to surface plasmon excitation at the Au and glass substrate interface.[20] It should be noted

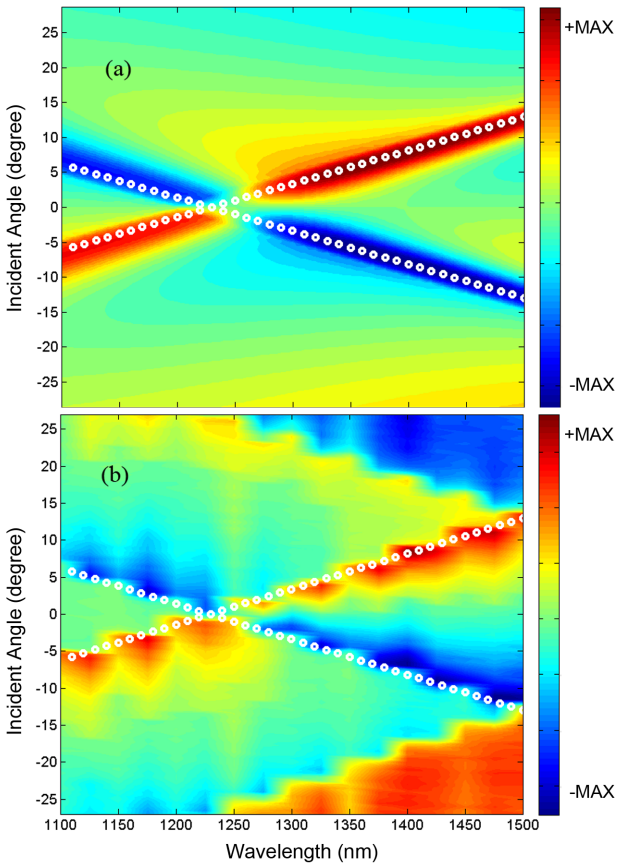

Figure 3. (a) Photon induced current density as calculated by the hydrodynamic model. The white open circles indicate the position of peak response. (b) Measured photon induced voltage as a function of incident angle and wavelength. The white open circles from the simulation are superimposed for comparison.

that the step-like transitions around 0 V are artifacts of the measurement due to noise floor.

To compare the measurement with the theoretical model, the photon induced voltage on the Au grating slab was measured from 1100 nm to 1500 nm at an interval of 50 nm and from 0° to 30° incidence at an interval of 1°. The incident power remained the same for all measurements. Figure 3(a) shows the photon induced current density as a function of incident angle and wavelength simulated with the hydrodynamic model. The white open circles indicate the positions of peak response for a given incident wavelength. This result is compared with the measurement as shown in Fig. 3(b). The staggered appearance is due to the limited wavelength samples. The agreement between the hydrodynamic model and the measurement can be observed. An increasing photon induced voltage as the wavelength increases from 1.25 μm to 1.6 μm, as observed in the experiment is also predicted by the model. Calculated responses at higher incident angles are found to have the same polarity as the measurement, but measurement shows a larger induced voltage at higher incident angles. This difference is possibly due to an increased surface roughness at the bottom of the grating due to ion beam etching. Since surface plasmon at the Au and substrate interface is attributed to the response at larger incident angles, the surface roughness can enhance the excitation efficiency. Figure 3(a) and 3(b) are normalized with their respective maximum. We did not compare calculations quantitatively with the experiment because the measurement were conducted in the pulse mode and the results are influenced by many factors such as impedance matching.[20] However, the calculation for a prism coupled flat Au film showed that the photon induced current density was over an order of magnitude lower for the same incident power, consistent with the observation reported by Ishihara et al.[8] Our results indicate that increasing the surface plasmon spatial variation enhances photon induced current. Finally, the voltage was also measured as a function of incident power at the wavelength of 1400 nm showing that it is a linear function of optical intensity, as indicated by Eq. (3).

In summary, the photon induced current on a Au grating slab is investigated numerically and experimentally. The calculated photon induced current as a function of incident angle and wavelength was found to be in qualitative agreement with the experimental measurements. In comparison with the momentum conservation approach, the nonlinear electron transport over a structured surface is also accounted for in this model. Hence the model reported here provides a pathway for the study of devices with more detailed photon-electron interactions.

This work has been supported by grants from NSF CAREER ECCS-0846415 and NSF MRI ECCS-0923541 and by DARPA under contract N66001-01-C-80345. The authors acknowledge helpful discussions with E. Graugnard and instrumentation development support by A. Spielgelman.

[1] L. Martín-Moreno, F. J. García-Vidal, H. J. Lezec, K. M. Pellerin, T. Thio, J. B. Pendry, and T. W. Ebbesen, Phys. Rev. Lett. **86**, 1114 (2001).
[2] W. L. Barnes, A. Dereux, and T. W. Ebbesen, Nature **424**, 824 (2003).
[3] A. Nahata, R. A. Linke, T. Ishi, and K. Ohashi, Opt. Lett. **28**, 423 (2003).
[4] A. S. Vengurlekar and T. Ishihara, Applied Physics Letters **87**, 091118 (2005).
[5] A. Lesuffleur, L. K. S. Kumar, and R. Gordon, Applied Physics Letters **88**, 261104 (2006).
[6] J. A. H. van Nieuwstadt, M. Sandtke, R. H. Harmsen, F. B. Segerink, J. C. Prangsma, S. Enoch, and L. Kuipers, Phys. Rev. Lett. **97**, 146102 (2006).
[7] N. Feth, S. Linden, M. W. Klein, M. Decker, F. B. P. Niesler, Y. Zeng, W. Hoyer, J. Liu, S. W. Koch, J. V. Moloney, and M. Wegener, Opt. Lett. **33**, 1975 (2008).
[8] T. Hatano, B. Nishikawa, M. Iwanaga, and T. Ishihara, Optics Express **16**, 8236 (2008).
[9] E. Kim, F. Wang, W. Wu, Z. Yu, and Y. R. Shen, Phys. Rev. B **78**, 113102 (2008).
[10] T. Xu, X. Jiao, and S. Blair, Opt. Express **17**, 23582 (2009).
[11] F. Kadlec, P. Kuzel, and J.-L. Coutaz, Opt. Lett. **30**, 1402 (2005).
[12] F. Kadlec, P. Kužel, and J.-L. Coutaz, Opt. Lett. **29**, 2674 (2004).
[13] G. H. Welsh and K. Wynne, Optics Express **17**, 2470 (2009).
[14] G. Sheroziya, JETP Lett **45**, 421 (1987).
[15] Y. Zeng, W. Hoyer, J. Liu, S. W. Koch, and J. V. Moloney, Phys. Rev. B **79**, 235109 (2009).
[16] J. E. Goff and W. L. Schaich, Phys. Rev. B **56**, 15421 (1997).
[17] N. Bloembergen, R. K. Chang, S. S. Jha, and C. H. Lee, Phys. Rev. **174**, 813 (1968).
[18] M. Corvi and W. L. Schaich, Phys. Rev. B **33**, 3688 (1986).
[19] A. Liebsch, *Electronic excitations at metal surfaces*, 1st ed. (Plenum Press, New York, 1997).
[20] See supplementary material at [URL will be inserted by AIP] for details regarding the derivations and discussions.

[21] "Multiphysics modeling and simulation software," .